Earth and Planetary Science Letters 292 (2010) 337–344

Contents lists available at ScienceDirect

Earth and Planetary Science Letters

journal homepage: www.elsevier.com/locate/epsl

Calcium isotopic fractionation between clinopyroxene and orthopyroxene from mantle peridotites

Shichun Huang *, Juraj Farkaš, Stein B. Jacobsen

Department of Earth and Planetary Sciences Harvard University 20 Oxford St., Cambridge MA 02138, United States

ARTICLE INFO

Article history:
Received 17 November 2009
Received in revised form 25 January 2010
Accepted 26 January 2010
Available online 23 February 2010

Editor: R.W. Carlson

Keywords:
Ca isotopes
stable isotopic fractionation
mantle geochemistry

ABSTRACT

We report the first observation of Ca isotopic fractionation between co-existing clinopyroxene and orthopyroxene from Kilbourne Hole and San Carlos mantle peridotites. The $^{44}Ca/^{40}Ca$ in orthopyroxenes is 0.36 to 0.75‰ heavier than that in the co-existing clinopyroxenes. Using these isotopic constraints and the relative proportions of major Ca-bearing minerals in the upper mantle, the estimated $^{44}Ca/^{40}Ca$ of the upper mantle is 1.05 ± 0.04‰ heavier relative to NIST SRM 915a. This is slightly higher than our average for basalts (0.97 ± 0.04‰ heavier relative to NIST SRM 915a). Combined with published $^{44}Ca/^{40}Ca$ data on low temperature Ca-bearing minerals (calcite, aragonite and barite), we infer that the inter-mineral fractionation of Ca isotopes at both low- and high temperatures is primarily controlled by the strength of Ca–O bond. Accordingly, the mineral with a shorter Ca–O bond and a smaller Ca coordination number (i.e., stronger Ca–O bond) yields a heavier Ca isotopic ratio (i.e., higher $^{44}Ca/^{40}Ca$). Since stable isotopes of major elements, such as Ca and Mg, exhibit small fractionations during igneous processes, the estimate of stable isotopic compositions of the bulk differentiated planetary bodies, including the Earth and the Moon, needs to take into account the relative proportions of major rock-forming minerals and their respective isotopic signatures.

1. Introduction

With the advancement of modern analytical techniques, non-traditional stable isotopes of Mg, Si, Ca and Fe, which were previously not believed to fractionate during magmatic processes, have become powerful tools in the fields of cosmochemistry (e.g., Georg et al., 2007; Fitoussi et al., 2008; Chakrabarti and Jacobsen, 2009) and high temperature geochemistry (e.g., Williams et al., 2004; Teng et al., 2008; Dauphas et al., 2009). As the fifth most abundant element in the Earth, Ca has six isotopes (^{40}Ca, ^{42}Ca, ^{43}Ca, ^{44}Ca, ^{46}Ca and ^{48}Ca), making it a geochemical and cosmochemical tracer with considerable potential (e.g., DePaolo, 2004). With the exception of H and He, Ca has the largest relative mass difference ($\Delta m/m = 20\%$) between the heaviest and the lightest isotopes. Thus, similar to stable isotopic studies of Si, Mg and Fe (e.g., Georg et al., 2007; Dauphas et al., 2009), the comparison of Ca isotopic ratios between the Earth and other planetary bodies, including the Moon, could yield important information regarding the early evolution of the Solar System and the origin of the Earth–Moon system (e.g., Simon and DePaolo, 2010). Knowledge of the Ca isotopic ratio in the Earth's mantle is also critical in investigating the chemical and isotopic evolution of seawater through geological time, as several lines of evidence suggest that the chemistry of the Archean and Paleoproterozoic oceans was strongly "mantle-buffered" due to massive circulation of seawater via oceanic crust and submarine hydrothermal systems (e.g., Veizer, 1982; Jacobsen and Kaufman, 1999).

Previous Ca isotopic studies have focused mostly on modern and ancient marine carbonates and sulphates, documenting large and systematic isotopic variations (e.g., DePaolo, 2004; Heuser et al., 2005; Kasemann et al., 2005; Farkaš et al., 2007; Griffith et al., 2008a), yet detailed work on igneous rocks is fairly limited (Russell et al., 1978; Skulan and DePaolo, 1999; DePaolo, 2004; Amini, 2007; Amini et al., 2009a, b). Russell et al. (1978) presented the first and the most extensive Ca isotopic study that covered a wide range of igneous rocks from the inner Solar System. More recently, DePaolo (2004) showed ~0.7‰ variation in $^{44}Ca/^{40}Ca$ in oceanic basalts (see his Fig. 5). Amini et al. (2009b) reported ~0.5‰ variation in $^{44}Ca/^{40}Ca$ in a series of silicate rocks, including both felsic and ultramafic rocks. Huang et al. (2009a) reported that Makapuu-stage Koolau lavas have slightly lower $^{44}Ca/^{40}Ca$ (by 0.2‰) than other Hawaiian tholeiitic lavas. The observed $^{44}Ca/^{40}Ca$ variation in basalts may be interpreted either as a result of recycling ancient carbonate into the mantle (Fig. 15 of DePaolo, 2004; Huang et al., 2009a), or due to the fractionation of stable Ca isotopes during igneous processes. In order to constrain the Ca isotopic composition of the Earth's mantle and to investigate the possible Ca isotopic fractionation during igneous process, we report $^{44}Ca/^{40}Ca$ measurements on a series of terrestrial igneous rocks, including two nephelinites from Oslo Rift (Norway), six Hawaiian shield stage tholeiites (USA), one dunite (DTS-1) from Twin Sisters (Washington, USA), and clinopyroxene and orthopyroxene separates

* Corresponding author. Tel.: +1 617 496 7393.
E-mail address: huang17@fas.harvard.edu (S. Huang).

0012-821X/$ – see front matter © 2010 Elsevier B.V. All rights reserved.
doi:10.1016/j.epsl.2010.01.042

Table 1
Ca isotopic ratios in selected mantle minerals and basalts.

	$\delta^{44/40}Ca$[a]	$2\sigma_{(m)}$[b]	$\delta^{42/40}Ca$[a]	$2\sigma_{(m)}$[b]	$\delta^{44/42}Ca$[a]	$2\sigma_{(m)}$[b]	Sample form	Acid leaching
Kilbourne Hole, New Mexico, USA								
Clinopyroxene								
	0.94		0.47		0.45		Crystals	Yes
	1.00		0.51		0.49		Crystals	Yes
	0.88		0.44		0.44		Crystals	Yes
	0.97		0.55		0.41		Crystals	Yes
	1.05		0.65		0.40		Crystals	Yes
	1.04		0.59		0.44		Crystals	Yes
	0.98		0.57		0.41		Crystals	Yes
Average	0.98	0.04	0.54	0.05	0.43	0.02		
Orthopyroxene								
	1.63		0.83		0.79		Crystals	Yes
	1.77		0.90		0.87		Crystals	Yes
	1.84		1.01		0.84		Crystals	Yes
	1.68		0.96		0.72		Crystals	Yes
Average	1.73	0.09	0.93	0.08	0.81	0.07		
San Carlos, Arizona, USA								
Clinopyroxene								
	1.11		0.58		0.53		Powdered crystals	Yes
	1.05		0.50		0.54		Powdered crystals	Yes
	1.02		0.58		0.43		Powdered crystals	Yes
	1.09		0.60		0.49		Powdered crystals	Yes
	1.03		0.51		0.52		Powdered crystals	No
	0.95		0.41		0.54		Powdered crystals	No
	1.01		0.62		0.39		Powdered crystals	No
Average	1.04	0.04	0.54	0.06	0.49	0.04		
Orthopyroxene								
	1.51		0.77		0.73		Powdered crystals	Yes
	1.41		0.82		0.59		Powdered crystals	Yes
	1.35		0.79		0.56		Powdered crystals	Yes
	1.30		0.66		0.66		Powdered crystals	Yes
	1.45		0.79		0.66		Powdered crystals	Yes
Average	1.40	0.07	0.77	0.06	0.64	0.06		
Orthopyroxene								
	1.16		0.56		0.60		Powdered crystals	No
	1.15		0.53		0.62		Powdered crystals	No
	1.31		0.70		0.61		Powdered crystals	No
Average	1.21	0.10	0.60	0.10	0.61	0.01		
Hawaii, USA								
Mauna Kea								
SR 687	0.88						Powder	No
	0.90		0.39	0.21	0.51	0.17	Powder	No
Average	0.89	0.13						
SR700	0.94		0.50		0.43		Powder	No
	0.89		0.40		0.48		Powder	No
	1.00		0.51		0.49		Powder	No
Average	0.94	0.06	0.47	0.07	0.47	0.04		
SR685	1.03		0.51		0.52		Powder	No
	0.90		0.49		0.41		Powder	No
Average	0.97	0.13	0.50	0.21	0.47	0.17		
Mahukona								
72-1	1.03	0.13	0.51	0.21	0.53	0.17	Powder	No
72-5	0.91	0.13	0.46	0.21	0.43	0.17	Powder	No
Kilauea								
BHVO-1	0.88						Powder	No
	1.04		0.51		0.53		Powder	No
	1.08		0.64		0.44		Powder	No
Average	1.00	0.12	0.58	0.21	0.49	0.17		
Nephelinites from Oslo Rift, Norway								
S36	0.94	0.13					Rock chip	No
S01	1.05		0.58		0.46		Rock chip	No
	1.07		0.60		0.47		Rock chip	No
Average	1.06	0.13	0.59	0.21	0.47	0.17		
All basalt average								
	0.97	0.04	0.51	0.04	0.48	0.02		
Twin Sisters Dunite								
DTS-1	1.57		0.76		0.81		Powder	No
	1.68		0.83		0.84		Powder	No
	1.53		0.77		0.76		Powder	No
Average	1.59	0.09	0.79	0.04	0.80	0.05		

[a] $\delta^{x/y}Ca = [(^{x}Ca/^{y}Ca_{sample}/^{x}Ca/^{y}Ca_{SRM915a}) - 1] * 1000$; where $^{44}Ca/^{40}Ca_{SRM915a} = 0.021549$, $^{44}Ca/^{42}Ca_{SRM915a} = 3.2274$ and $^{42}Ca/^{40}Ca_{SRM915a} = 0.006677$.

[b] If three or more analyses of one sample are available, the errors are 2 standard error of the mean. If only one or two analyses of one sample are available, the error is taken as 0.13 for $\delta^{44/40}Ca$, 0.21 for $\delta^{42/40}Ca$ and 0.17 for $\delta^{44/42}Ca$. These reflect the external reproducibility of our analyses on SRM 915a and seawater (Table S3).

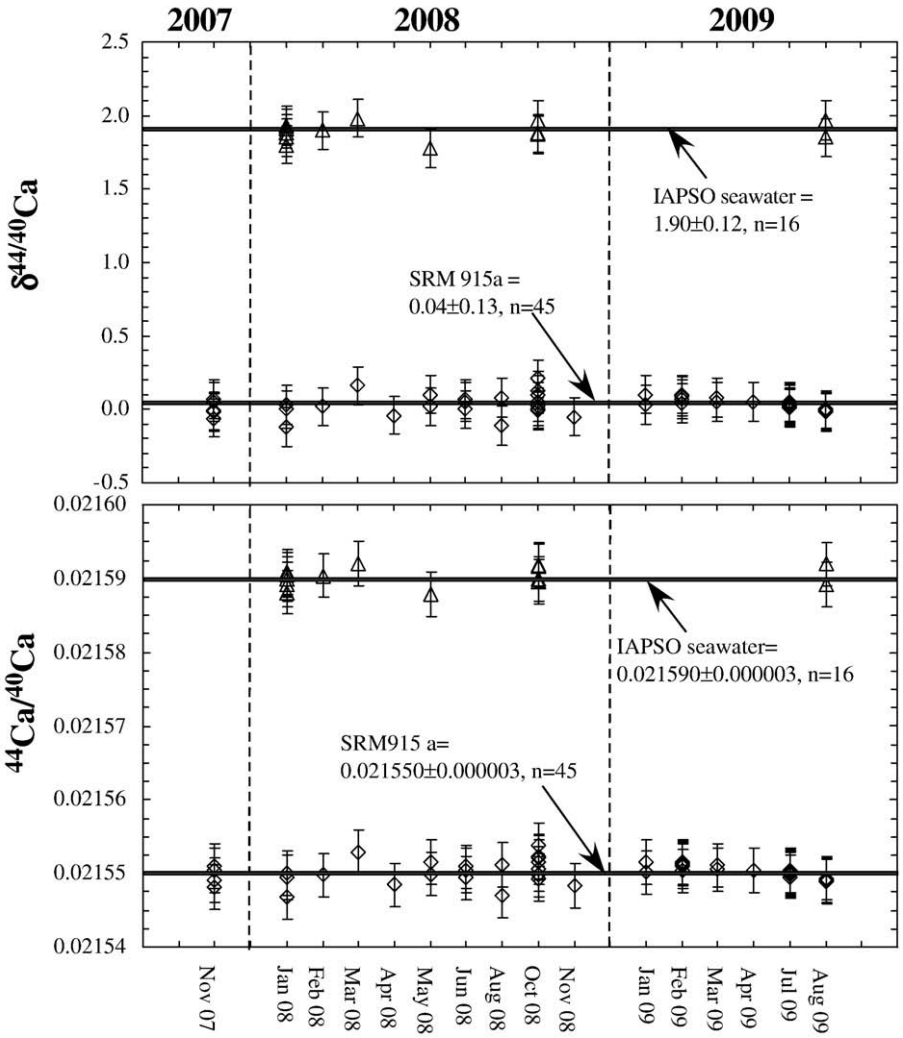

Fig. 1. Long-term (over 22 months) $\delta^{44/40}$Ca and ^{44}Ca/^{40}Ca measurements of NIST SRM 915a and seawater (IAPSO Atlantic seawater) obtained with the IsoProbe-T at Harvard University. The cited errors on each single analysis are 2 standard deviations of multiple analyses of NIST SRM 915a ($n=45$) and IAPSO seawater ($n=16$) (Table S3). Note that we did not observe any long-term ^{44}Ca/^{40}Ca drift in our measured standard samples (NIST SRM 915a and IAPSO seawater).

from San Carlos (Arizona, USA) and Kilbourne Hole (New Mexico, USA) mantle peridotites (Table 1). The San Carlos mantle peridotite was collected by S. B. Jacobsen, and its major element compositions were measured at Harvard University (Table S4). Clinopyroxene and orthopyroxene separates from Kilbourne Hole mantle peridotite were provided by J. Barr and T. L. Grove, and their major element compositions are given in Gaetani and Grove (1998).

2. Analytical method

A detailed description of our analytical procedure is given in the Supplemental material. We summarize the essentials here. Rock samples were dissolved in a mixture of 1:1 HNO_3–HF acids in Teflon beakers. An aliquot containing 10–20 μg Ca was moved into a pre-cleaned beaker and mixed with a ^{43}Ca–^{48}Ca double spike. After equilibration, the Ca fraction was separated from the silicate matrix by conventional chromatography, using PFA microcolumns filled with 250 μl cation exchange resin (BioRad AG50W-X12) and HCl acid. About 5 μg purified Ca was loaded on a side filament of a triple-filament assembly with Re ribbons. The whole procedural Ca blank was less than 25 ng. The Ca isotopic compositions were measured at Harvard University with an IsoProbe-T TIMS using a two-sequence method. The first sequence collected masses 40 to 44 and the second 44 to 48. The mass-dependent Ca isotopic variations, expressed as $\delta^{44/40}$Ca relative to NIST SRM 915a standard ($\delta^{44/40}Ca = [(^{44}Ca/^{40}Ca_{SAMPLE}/^{44}Ca/^{40}Ca_{SRM915a}) - 1] * 1000$, with $^{44}Ca/^{40}Ca_{SRM915a} = 0.021549$)[1], were determined by a ^{43}Ca–^{48}Ca double spiking technique using an offline data reduction with an exponential law (Heuser et al., 2002). The long-term averages of $\delta^{44/40}$Ca measurements of NIST 915a and IAPSO seawater are 0.04 ± 0.13 ($n=45, 2\sigma$) and 1.90 ± 0.12 ($n=16, 2\sigma$), respectively (Fig. 1; Table S3).

3. Experiments

1. In order to investigate whether our HNO_3–HF digestion procedure introduces any Ca isotopic fractionation because of the possible precipitation of insoluble CaF_2, an aliquot of IAPSO seawater containing ~40 μg Ca was processed using the same HNO_3–HF digestion protocol as used for basalts and mineral separates (see Supplemental material). Then an aliquot containing 10 μg Ca was moved to another pre-cleaned beaker and mixed with a ^{43}Ca–^{48}Ca double spike before column chemistry.

[1] We note that as a tradition, in many publications the reported $\delta^{44/40}$Ca values are followed by a "‰" symbol. However, this per mil symbol is redundant following the definition of δ notation, and it is misleading to readers who are not familiar with Ca isotopic research.

2. Secondary carbonate phases may precipitate on mineral surfaces and along cracks in the silicate minerals when mantle xenoliths are exposed on the surface of the Earth (e.g., Ionov, 1998). Thus, the precipitated carbonates may bias the Ca isotopic ratios of the measured silicate minerals, especially if they are Ca-poor such as orthopyroxenes. In order to investigate this effect, we analyzed the Ca isotopic ratios in acid-leached and unleached clinopyroxene and orthopyroxene separates from San Carlos mantle xenolith. In the leaching experiments, powdered San Carlos clinopyroxene (13 mg) and orthopyroxene (43 mg) were leached at room temperature with 6 ml 1 N HCl overnight before they were dissolved with HNO_3–HF.

4. Results

4.1. Experiment results

4.1.1. Effect of HNO_3–HF digestion on IAPSO seawater

Two measurements of IAPSO seawater processed with HNO_3–HF digestion procedure were made on Oct. 8, 2008, and yield $\delta^{44/40}$Ca of 1.88 and 1.97, indistinguishable from other measurements on IAPSO seawater (1.90 ± 0.12, 2σ) which were not processed with HNO_3–HF digestion procedure (Table S3b). Our HNO_3–HF digestion procedure does not introduce any measurable Ca isotopic fractionation.

4.1.2. Effect of acid leaching on Ca isotopic analysis

The unleached San Carlos orthopyroxene yields $\delta^{44/40}$Ca lower than acid-leached San Carlos orthopyroxene: three analyses of the unleached San Carlos orthopyroxene yield $\delta^{44/40}$Ca of 1.16, 1.15 and 1.31, with an average of 1.21 ± 0.10 ($2\sigma_m$), and five analyses on acid-leached San Carlos orthopyroxene yield $\delta^{44/40}$Ca of 1.51, 1.41, 1.35, 1.30 and 1.45, with an average of 1.40 ± 0.07 ($2\sigma_m$) (Table 1). In contrast, acid-leached and unleached San Carlos clinopyroxenes have similar $\delta^{44/40}$Ca: three analyses of unleached San Carlos clinopyroxene yield $\delta^{44/40}$Ca of 1.03, 0.95 and 1.01, with an average of 1.00 ± 0.07 ($2\sigma_m$), and four analyses of acid-leached San Carlos clinopyroxene yield $\delta^{44/40}$Ca of 1.11, 1.05, 1.02 and 1.09, with an average of 1.07 ± 0.04 ($2\sigma_m$). Since carbonates, in general, have $\delta^{44/40}$Ca lower than those in basalts and peridotites (DePaolo, 2004; Heuser et al., 2005; Kasemann et al., 2005; Farkaš et al., 2007; Griffith et al., 2008a; Amini et al., 2009b), the lower $\delta^{44/40}$Ca in unleached San Carlos orthopyroxene most likely reflects Ca contribution from carbonates precipitated on the mineral surface. Because clinopyroxenes have ~20% CaO and orthopyroxenes have ~0.9% CaO (e.g., Galer and O'Nions, 1989), it is expected that carbonates that precipitated on the mineral surfaces will affect the Ca isotopic ratio of orthopyroxene but not clinopyroxene. Therefore, in Table 1 we average the Ca isotopic measurements on both acid-leached and unleached San Carlos clinopyroxene. Ca isotopic measurements on Kilbourne Hole clinopyroxene and orthopyroxene were obtained on acid-leached samples. Since the analyzed Hawaiian basalts have CaO content of 10% to 12% (e.g., Huang et al., 2009b) and the two Oslo Rift nephelinites have CaO contents of ~19% (Anthony et al., 1989), Ca isotopic measurements on these samples were obtained on unleached samples. We ignore the result of unleached San Carlos orthopyroxene in our following discussion.

4.2. $\delta^{44/40}$Ca in silicate rocks and mineral separates

The average $\delta^{44/40}$Ca of six Hawaiian shield basalts and two Oslo Rift nephelinites is 0.97 ± 0.04 ($2\sigma_m$), and San Carlos and Kilbourne Hole clinopyroxenes yield $\delta^{44/40}$Ca of 1.04 ± 0.04 and 0.98 ± 0.04 ($2\sigma_m$), respectively (Table 1; Fig. 2). Even though the CaO contents in our analyzed basalts and clinopyroxenes range from 10% to 21% (Anthony et al., 1989; Gaetani and Grove, 1998; Huang et al., 2009b; Table S4), their $\delta^{44/40}$Ca are indistinguishable from each other. In contrast, mantle orthopyroxenes have much higher $\delta^{44/40}$Ca: San Carlos and Kilbourne Hole orthopyroxenes yield $\delta^{44/40}$Ca of 1.40 ± 0.07 ($2\sigma_m$) and 1.73 ± 0.09 ($2\sigma_m$), respectively (Table 1; Fig. 2).

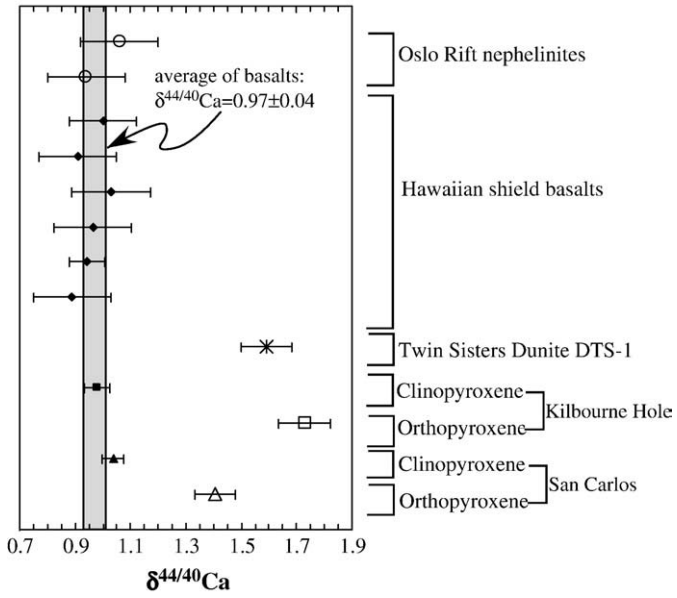

Fig. 2. $\delta^{44/40}$Ca in Hawaiian shield tholeiites, Oslo Rift nephelinites, Twin Sisters dunite DTS-1, and mineral separates from San Carlos and Kilbourne Hole mantle peridotites. The grey bar shows the average $\delta^{44/40}$Ca, with 2 standard error of the mean, of six Hawaiian basalts and two Oslo Rift nephelinites. Each point represents the average value of all the measurements of that particular sample. The unleached San Carlos orthopyroxene is not included.

The USGS reference material DTS-1 also has high $\delta^{44/40}$Ca of 1.59 ± 0.09 ($2\sigma_m$) (Table 1; Fig. 2). This high $\delta^{44/40}$Ca is confirmed with independent TIMS analysis by Amini et al. (2009b) who reported $\delta^{44/40}$Ca in DTS-1 of 1.49 ± 0.06. DTS-1 is a dunite from the Twin Sisters area, Hamilton, Washington, which contains primarily olivine (99%), orthopyroxene, clinopyroxene and trace amounts of chromite and amphibole (Flanagan, 1967). Some olivines were serpentinized. So the observed high $\delta^{44/40}$Ca in DTS-1 might be a result of alteration, and further detailed work is required to investigate the origin of its high $\delta^{44/40}$Ca.

The $\delta^{44/40}$Ca does not show any correlation with raw ^{43}Ca/^{48}Ca or raw ^{40}Ca/^{48}Ca ratios, the latter two are not corrected for instrumental isotopic fractionation (Fig. S3). Consequently, the observed Ca isotopic difference is not a result of analytical artifacts due to isotopic fractionation on columns or non-optimal spiking conditions (see Supplemental material for a detailed discussion). Within error, all our analyzed samples plot along mass-dependent exponential fractionation lines in three Ca isotope plots ($\delta^{44/40}$Ca vs. $\delta^{42/40}$Ca and $\delta^{44/42}$Ca; Fig. 3), indicating excellent isotopic measurements that are not biased by isobaric interferences and a proper estimate of the error bars. The studied mantle peridotites were equilibrated at high temperatures, >900 °C (e.g., Galer and O'Nions, 1989; Bussod and Williams, 1991; Hamblock et al., 2007). Therefore, our result shows mass-dependent Ca isotopic fractionation between co-existing silicate minerals at fairly high temperatures.

5. Discussions

5.1. Ca isotopic fractionation at low and high temperatures

At low temperature, the fractionation of Ca isotopes between seawater and Ca-bearing minerals (calcite, aragonite and barite) has been well documented (e.g., Lemarchand et al., 2004; Gussone et al., 2005; Griffith et al., 2008b). It has been proposed that the observed Ca isotopic fractionation between seawater and a mineral is mostly controlled by precipitation kinetics, such as crystallization rate and temperature (e.g., Tang et al., 2008) or the saturation state of the solution with respect to Ca-bearing minerals (e.g., Lemarchand et al., 2004), but also by an equilibrium effect dependent on the length of the

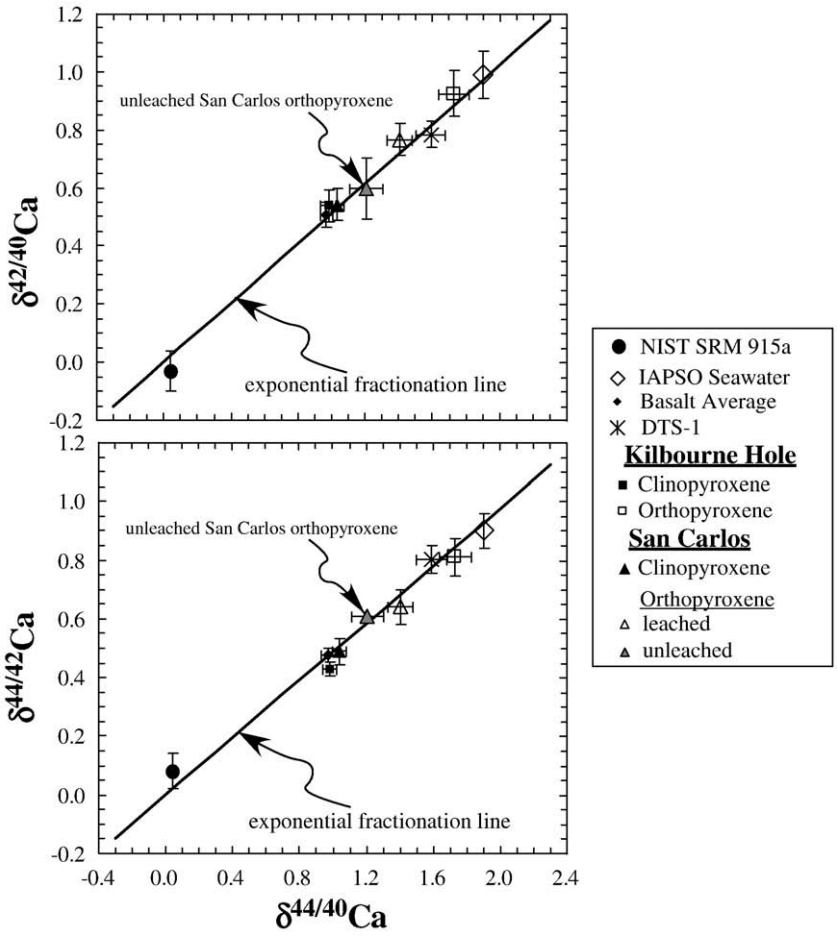

Fig. 3. $\delta^{44/40}$Ca vs. $\delta^{42/40}$Ca and $\delta^{44/42}$Ca in our measured samples. The theoretically calculated exponential fractionation lines (Hart and Zindler, 1989) are shown for comparison. Note that, within errors, all our analyzed samples plot on the exponential fractionation lines, indicating excellent isotopic measurement, not affected by isotopic interferences, and a proper estimate of the error bars. The δ^{44}Ca/^{40}Ca error bars on NIST SRM 915a and IAPSO seawater, and the δ^{44}Ca/^{42}Ca error bar on unleached San Carlos orthopyroxene are smaller than their symbols (Tables 1and S3).

Ca–O bond in the mineral; i.e., the shorter the Ca–O bond, the higher the $\delta^{44/40}$Ca in the mineral (Gussone et al., 2005; Griffith et al., 2008b; but also see Fantle and DePaolo, 2007 for a different point of view). In fact, the idea that at equilibrium conditions, a stronger bond tends to yield heavier stable isotopes has been discussed for both light elements (H, C and O, e.g., Chacko et al., 2001) and heavy elements (e.g., Cl, Cr and Fe, e.g., Schauble, 2004; Polyakov et al., 2007). This relationship for Ca isotopes is illustrated in Fig. 4a, where we show a negative correlation between the calculated $\delta^{44/40}$Ca and the estimated Ca–O bond length in calcite, aragonite and barite precipitates. The corresponding $\delta^{44/40}$Ca are calculated using the empirical Ca isotopic fractionation factor ($\alpha = {}^{44}Ca/{}^{40}Ca_{mineral}/{}^{44}Ca/{}^{40}Ca_{seawater}$) between a mineral and seawater, assuming $\delta^{44/40}Ca_{seawater} = 1.90$ (Table S3) and a temperature of 25 °C (Gussone et al., 2005; Griffith et al., 2008b). This negative correlation between $\delta^{44/40}$Ca and the Ca–O length (Fig. 4a) was proposed to reflect the effect of Ca–O bond strength on Ca isotopes in minerals. Specifically, the heavier Ca isotope is preferentially kept by stronger (i.e., shorter) Ca–O bond (Gussone et al., 2005; Griffith et al., 2008b). Accordingly, the Ca–O bond in calcite is shorter than that in aragonite (Fig. 4a), and thus it is ~60% stronger than in aragonite (Zheng, 1999). Consequently, the lattice structure of calcite would yield higher $\delta^{44/40}$Ca than that of aragonite, which is in agreement with the observations (Gussone et al., 2005).

At high temperature, the co-existing orthopyroxenes and clinopyroxenes from San Carlos and Kilbourne Hole peridotites also define a negative trend in a plot of $\delta^{44/40}$Ca vs. Ca–O length (Fig. 4b). Specifically, $\Delta^{44/40}Ca_{OPX-CPX}$, defined as $\delta^{44/40}Ca_{OPX}$–$\delta^{44/40}Ca_{CPX}$, is 0.75 ± 0.10 and 0.37 ± 0.08 in Kilbourne Hole and San Carlos mantle peridotites, respectively (Fig. 2; Table 1). Ca occupies the M2 site in clinopyroxene, with a coordination number of 8 and an average Ca–O length of 2.50 Å. In orthopyroxene, Ca also occupies the M2 site, with a coordination number of 6 and a much shorter Ca–O length of 2.15 Å (Smyth and Bish, 1988). Thus, the higher $\delta^{44/40}$Ca of orthopyroxenes could be explained by their relatively shorter Ca–O bond.

The observed Ca isotopic fractionation between co-existing orthopyroxene and clinopyroxene pairs can be qualitatively estimated by considering the different Ca–O bonding conditions in two minerals. The inter-mineral isotopic fractionation is proposed to be controlled by the bonding environment of the element of interest (e.g., Urey, 1947; Young et al., 2002; 2009). A simplified approach associating the equilibrium inter-mineral isotopic fractionation with its bonding environment can be found in Young et al. (2002; 2009), and we summarize the important points here. The inter-mineral (between orthopyroxene and clinopyroxene) Ca isotopic fractionation is given by:

$$\Delta^{44/40}Ca_{OPX-CPX} = \frac{1000}{24}\left(\frac{h}{k_b T}\right)^2\left(\frac{1}{m_{40}}-\frac{1}{m_{44}}\right)\left(\sum_j \frac{K_{f.j,OPX}}{4\pi^2}-\sum_j \frac{K_{f.j,CPX}}{4\pi^2}\right)$$

where m_{40} and m_{44} are the atomic masses of ^{40}Ca and ^{44}Ca, respectively; k_b is Boltzmann's constant (1.3806503×10^{-23} m^2 kg/s^2 K); h is Planck's constant (6.626068×10^{-34} m^2 kg/s); T is temperature in Kelvin; K_{fj} is

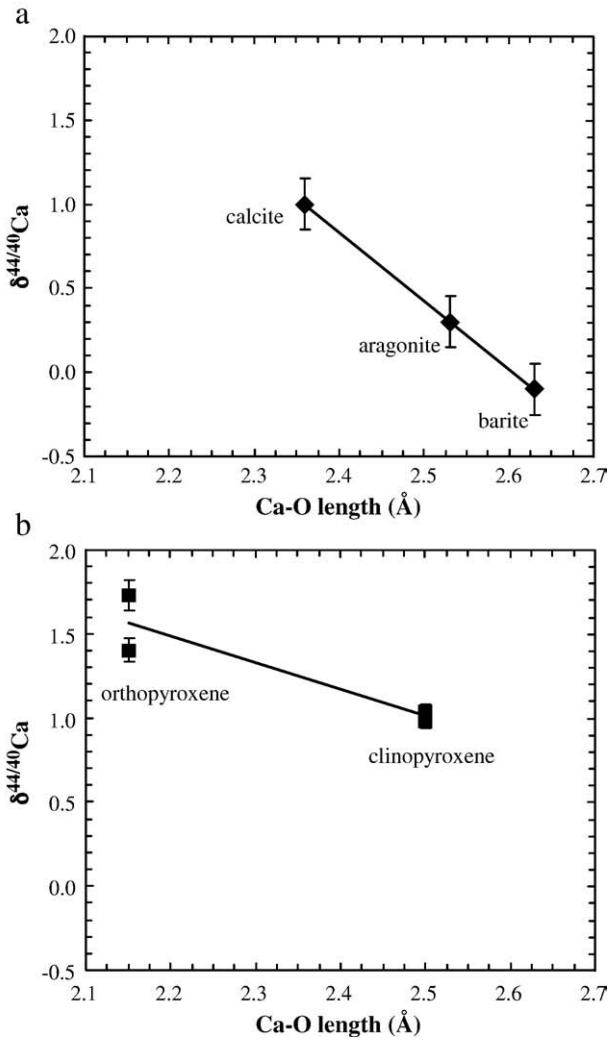

Fig. 4. $\delta^{44/40}$Ca vs. Ca–O bond length (Å) in (a) low temperature (25 °C) minerals (calcite, aragonite and barite) and (b) co-existing orthopyroxene and clinopyroxene from San Carlos and Kilbourne Hole mantle peridotites. $\delta^{44/40}$Ca in calcite, aragonite and barite are calculated using the $^{44}Ca/^{40}Ca_{mineral}/^{44}Ca/^{40}Ca_{seawater}$ from Gussone et al. (2005) and Griffith et al. (2008b) and assuming $\delta^{44/40}Ca_{seawater} = 1.90$ (Fig. 1; Table S3) and a temperature of 25 °C. The error bars on calcite, aragonite and barite are taken as ±0.15, which reflects the typical analytical uncertainty in these studies.

the force constant of a particular bond connecting Ca and O; and the summations are over all relevant Ca–O bonds (6 in orthopyroxene and 8 in clinopyroxene). Following the qualitative approach of Young et al. (2009), $K_{f,j}$ is treated as electrostatic in origin, and $K_{f,j}$ is given by:

$$K_{f,j} = \frac{S_{Ca} S_O e^2 (1-n)}{4\pi\varepsilon_o r^3_{Ca-O}}$$

where, ε_o is the electric constant (8.85418782×10^{-12} s^4 A^2/m^3 kg); e is the charge of an electron (1.60217646×10^{-18} C); r_{Ca-O} is Ca–O bond length, with $r_{Ca-O,\,CPX} = 2.50\times10^{-10}$ m and $r_{Ca-O,\,OPX} = 2.15\times10^{-10}$ m; n is the exponent in the Born–Mayer formulation for ion repulsion, which ranges from 5 to 12 for different types of bonding (c.f., Wulfsberg, 1991). S_{Ca} and S_O are mean bond strengths of Ca and O, defined as: $S_{Ca} = \frac{Z_{Ca}}{\nu_{Ca}}$ and $S_O = \frac{Z_O}{\nu_O}$, where Z_{Ca} and Z_O are the valences of Ca and O, and ν_{Ca} and ν_O are the coordination numbers for Ca and O.

The equations mentioned above explicitly show that a shorter Ca–O bond and a smaller Ca coordination number correspond to a higher force constant, $K_{f,j}$, i.e., stronger Ca–O bond. Since the Ca–O bond in orthopyroxene is shorter (2.15 Å) than that in clinopyroxene (2.50 Å), and the coordination number of Ca in orthopyroxene (6) is smaller than that in clinopyroxene (8), it is predicted that at a given temperature orthopyroxene tends to yield higher $^{44}Ca/^{40}Ca$ than co-existing clinopyroxene. Using $n = 12$, and the average pyroxene equilibration temperatures of San Carlos and Kilbourne Hole mantle peridotites (1022 ± 34 °C and 1003 ± 58 °C, respectively, e.g., Galer and O'Nions, 1989; Bussod and Williams, 1991; Hamblock et al., 2007), the predicted equilibrium $\Delta^{44/40}Ca_{OPX-CPX}$ is 0.18–0.20. This value is smaller than the measured $\Delta^{44/40}Ca_{OPX-CPX}$ in leached pyroxene pairs from San Carlos and Kilbourne Hole mantle peridotites (0.37–0.75). But it is close to the isotopic fractionation observed in the unleached pyroxene pair from San Carlos (Table 1). However, we note that this qualitative approach has "severe limitations" (Young et al., 2009), and it may not fully and accurately describe the equilibrium inter-mineral isotopic fractionation. A more sophisticated model, such as the approach using lattice dynamics for Mg isotopic fractionation by Schauble (in review), is currently not available for equilibrium Ca isotopic fractionation. Nevertheless, the concept discussed above and its preliminary results are in general agreement with our observation, as both show that orthopyroxene has higher $\delta^{44}Ca/^{40}Ca$ than the co-exiting clinopyroxene.

Rather large (up to 7‰) $^{44}Ca/^{40}Ca$ variation has been measured in a chemical and thermal diffusion experimental charge using basalt and rhyolite, which was interpreted as a result of both thermal and chemical diffusions, i.e., kinetic isotopic effect (Richter et al., 2009). Further, Young et al. (2009) observed measurable δ^{25}Mg difference among olivine, spinel, clinopyroxene and orthopyroxene separates from two San Carlos mantle peridotites (but see also Handler et al., 2009; Yang et al., 2009), and concluded that the $\Delta^{25}Mg_{CPX-OL}$ and $\Delta^{25}Mg_{OPX-OL}$ are too high to be explained as a result of equilibrium isotopic fractionation. Consequently, they expected that Mg isotopic disequilibrium controlled by kinetic processes is important in clinopyroxene and orthopyroxene from San Carlos mantle peridotite. Although we are not able to fully exclude the possibility that the observed $\Delta^{44/40}Ca_{OPX-CPX}$ in San Carlos and Kilbourne Hole mantle peridotites reflect kinetic isotopic effect, we note that:

1. The pyroxene pairs in our study are from San Carlos and Kilbourne Hole mantle peridotites, which appear to have achieved complete chemical equilibration. For example, Galer and O'Nions (1989) argued that "the observed partitioning of elements between the principal mineral phases suggests that complete chemical equilibration occurred between phases once the bulk rock chemistry was established".
2. If a kinetic Ca isotopic effect is important in pyroxene pairs from mantle peridotites, these mantle mineral grains should show compositional and isotopic zoning. Our preliminary electron probe analysis on San Carlos pyroxenes does not reveal any observable compositional zoning. An in-situ Ca isotopic analysis (Rollion-Bard et al., 2007) on these pyroxene grains is required to further address this question.
3. Ca^{2+} has a larger ionic radius than Mg^{2+}; so Ca diffuses slower than Mg. Thus, a metasomatic process would not affect Ca as much as Mg.

Regardless of the nature of the observed inter-mineral Ca isotopic fractionation (equilibrium vs. kinetic isotopic fractionation), our observation introduces an additional aspect that needs to be considered in future estimates of the Ca isotopic composition of the bulk Earth and other differentiated planetary bodies (e.g., Simon and DePaolo, 2010). A similar effect may also be expected for Mg, Si and Fe isotopes (e.g., Fig. 2 of Young et al., 2009). Consequently, the comparison of stable isotopic ratios of Mg, Si, Ca and Fe between differentiated planetary bodies, such as the Earth and the Moon, and chondrites needs to be done with extra caution and taking into account the observed inter-mineral isotopic fractionation (e.g., Georg et al., 2007; Dauphas et al., 2009; Young et al., 2009; Simon and DePaolo, 2010).

5.2. The $^{44}Ca/^{40}Ca$ ratio of the Earth's upper mantle

There is large $^{44}Ca/^{40}Ca$ variation in published data on oceanic basalts. For example, Zhu and MacDougall (1998) reported three MORB samples having $\delta^{44/40}Ca$ of 1.21–1.36 (after re-normalization to $\delta^{44/40}Ca_{seawater} = 1.90$). Including the published data from Skulan et al. (1997), DePaolo (2004) showed that $\delta^{44}Ca/^{40}Ca$ in oceanic basalts range from 0.67 to 1.34 (after re-normalization to $\delta^{44/40}Ca_{seawater} = 1.90$). Due to this large isotopic variability and the fact that Ca isotopes fractionate during igneous process (this study), the upper mantle $^{44}Ca/^{40}Ca$ may be better reconstructed using the Ca isotopic measurement on mantle peridotites. Among the four major upper mantle minerals, clinopyroxene, orthopyroxene, olivine and spinel, the latter two contain only a negligible amount of CaO. Assuming that the studied minerals (clinopyroxene and orthopyroxene) are representative of the upper mantle, our $\delta^{44/40}Ca$ measurements allow an estimate of the Ca isotopic composition of the upper mantle. The mantle $\delta^{44/40}Ca$ depends on the relative proportions of clinopyroxene and orthopyroxene. This is highlighted in Fig. 5 where the proportion of olivine + spinel is fixed at 55%, and the proportion of clinopyroxene + orthopyroxene is at 45%. Using the upper mantle mineral assemblage, i.e., 13% to 18% clinopyroxene–32% to 27% orthopyroxene (Salters and Stracke, 2004; Workman and Hart, 2005), our estimate of the upper mantle $\delta^{44/40}Ca$ is 1.05 ± 0.04 (ranging from 1.02 to 1.08; Fig. 5). This mantle $\delta^{44/40}Ca$ estimate is slightly higher (by 0.08 ± 0.06) than the average $\delta^{44/40}Ca$ of our measured basalts (0.97 ± 0.04), which is consistent with the result from Amini et al. (2009a, b) who analyzed the bulk mantle peridotites. Using the published data on igneous rocks from Skulan et al. (1997), DePaolo (2004) implied that the average $\delta^{44/40}Ca$ of the Earth's mantle should be close to $\sim 1.00 \pm 0.15$ (after re-normalization to $\delta^{44/40}Ca_{seawater} = 1.90$), which is within error to our estimate of 1.05 ± 0.04.

Due to the limited number of samples analyzed with the precision and accuracy reported here, we by no means regard our upper mantle $\delta^{44/40}Ca$ estimate as the final. Rather, because of the measurable $\delta^{44/40}Ca$ variation in oceanic basalts and the inter-mineral Ca isotopic fractionation in mantle peridotites, we argue that the representative Ca isotopic composition of the mantle now becomes a scientific question and a substantially large number of well selected samples need to be analyzed in order to precisely and fully characterize the upper mantle Ca isotopic composition.

6. Conclusions

1. We found that $^{44}Ca/^{40}Ca$ in orthopyroxenes are 0.36–0.75‰ heavier than those in co-existing clinopyroxenes in mantle peridotites, suggesting that Ca isotopes can be fractionated during igneous processes via combined effects of the Ca–O bond strength in silicate minerals and their equilibrium crystallization temperature. Specifically, the mineral with a shorter Ca–O bond and a lower Ca coordination number (i.e., stronger bond) yields a heavier Ca isotopic ratio (i.e., higher $^{44}Ca/^{40}Ca$).
2. Based on our $^{44}Ca/^{40}Ca$ measurements of clinopyroxene and orthopyroxene in mantle peridotites, the upper mantle $\delta^{44/40}Ca$ is estimated at 1.05 ± 0.04 (ranging from 1.02 to 1.08), very close to the original estimate by DePaolo (2004), but slightly higher than our average $\delta^{44/40}Ca$ for basalts (0.97 ± 0.04).
3. Finally, since stable isotopes of Ca are fractionated during igneous processes, the future estimates of Ca isotopic composition of the bulk differentiated planetary bodies, including the Earth and the Moon, need to take into account the relative proportions of major rock-forming minerals and their respective isotope signatures.

Acknowledgements

This work was partially supported by NSF award EAR-0951487, NASA Cosmochemistry award NNX07AF86G and Earth System Program at CIFAR (Canadian Institute for Advanced Research). Clinopyroxene and orthopyroxene separates from Kilbourne Hole mantle peridotite were provided by J. Barr and T. L. Grove. We thank A. Déjeant, M. I. Petaev, R. Chakrabarti and G. Yu for help with the analyses. We thank M. Hirschmann, M. Humayun, S. Singletary, M. van Kan and W. van Westrenen for discussion. Reviews from M. Amini, T. Bullen, E. Schauble,

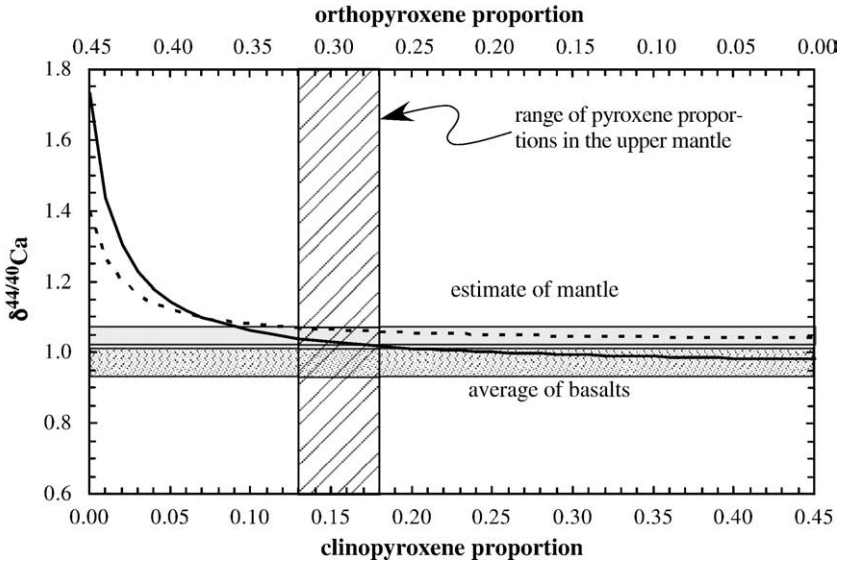

Fig. 5. $\delta^{44/40}Ca$ as a function of the relative proportion of clinopyroxene in the upper mantle. The proportion of olivine + spinel in the upper mantle is assumed to be 55%, and the proportions of clinopyroxene and orthopyroxene are varied. The solid line represents mixing line between $\delta^{44/40}Ca_{CPX} = 0.98$, $[CaO]_{CPX} = 20.50\%$ and $\delta^{44/40}Ca_{OPX} = 1.73$, $[CaO]_{OPX} = 0.75\%$ (Kilbourne Hole, Tables S1 and S4), and the dashed line represents mixing line between $\delta^{44/40}Ca_{CPX} = 1.04$, $[CaO]_{CPX} = 21.43\%$ and $\delta^{44/40}Ca_{OPX} = 1.40$, $[CaO]_{OPX} = 1.03\%$ (San Carlos, Tables S1 and S4). The vertical slashed area represents the range of clinopyroxene proportion (13–18%) in the upper mantle from Salters and Stracke (2004) and Workman and Hart (2005). The horizontal grey area represents our estimated upper mantle Ca isotopic ratio ($\delta^{44/40}Ca = 1.02$–1.08; with an average of 1.05 ± 0.04), with the upper mantle mineral assemblages ranging from 13% clinopyroxene–32% orthopyroxene to 18% clinopyroxene–27% orthopyroxene. Since Ca budget and $\delta^{44/40}Ca$ in peridotite are dominated by clinopyroxene, the error on $\delta^{44/40}Ca$ along the mixing line is dominated by the analytical $\delta^{44/40}Ca$ error of clinopyroxene (± 0.04; Table 1). Consequently, we cite ± 0.04 as the error of the estimated mantle $\delta^{44/40}Ca$. The horizontal dotted area represents average $\delta^{44/40}Ca$ in basalts (this study) from Fig. 2 and Table 1.

J. I. Simon and several anonymous reviewers are highly appreciated, and we thank R. Carlson for his excellent editorial handling.

Appendix A. Supplementary data

Supplementary data associated with this article can be found, in the online version, at doi:10.1016/j.epsl.2010.01.042 (Russell and Papanastassiou, 1978; Tuttas and Schwieters, 2002).

References

Amini, M. 2007. The role of high- and low-temperature ocean crust alteration for the marine calcium budget, Doctoral thesis, Christian-Albrechts-Universitaet zu Kiel, pp 93.

Amini, M., Holmden, C., Jochum, K.P., 2009. The Ca isotope composition of bulk Earth: revisited. Geochim. Cosmochim. Acta. 73, A36.

Amini, M., Eisenhauer, A., Böhm, F., Holmden, C., Kreissig, K., Hauff, F., Jochum, K.P., 2009. Calcium isotopes ($\delta^{44/40}$Ca) in MPI-DING reference glasses, USGS rock powders and various rocks: evidence for Ca isotope fractionation in terrestrial silicates. Geostandards Newsl. 33, 231–247.

Anthony, E.Y., Segalstad, T.V., Neumann, E.-R., 1989. An unusual mantle source region for nephelinites from the Oslo Roft, Norway. Geochim. Cosmochim. Acta. 53, 1067–1076.

Bussod, G.Y.A., Williams, D.R., 1991. hermal and kinematic model of the southern Rio Grande rift: inference from crustal and mantle xenoliths from Kilbourne Hole, New Mexico. Tectonophysics 197, 373–389.

Chacko, T., Cole, D.R., Horita, J., 2001. Equilibrium oxygen, hydrogen and carbon isotope fractionation factors applicable to geologic systems. Rev. Miner. Geochem. 43, 1–82.

Chakrabarti, R., Jacobsen, S.B., 2009. A combined silicon and magnesium isotopic study of bulk meteorites and the Earth. Lunar Planet. Sci. XL, Abstract #2089.

Dauphas, N., Craddock, P.R., Asimov, P.D., Bennett, V., Nutman, A.P., Ohnenstetter, D., 2009. Iron isotopes may reveal the redox conditions of mantle melting from Archean to Present, Earth Planet. Sci. Lett. 288, 255–267. doi:10.1016/j.epsl.2009.09.029.

DePaolo, D.J., 2004. Calcium isotopic variations produced by biological, kinetic, radiogenic and nucleosynthetic processes. In: Rosso, Jodi (Ed.), Chapter in REVIEWS in MINERALOGY and GEOCHEMISTRY, 55, pp. 255–288.

Fantle, M.S., DePaolo, D.J., 2007. Ca isotopes in carbonate sediment and pore fluid from ODP Site 807A: the Ca^{2+}(aq)-calcite equilibrium fractionation factor and calcite recrystallization rates in Pleistocene sediments. Geochim. Cosmochim. Acta. 71, 2524–2546. doi:10.1016/j.gca.2007.03.006.

Farkaš, J., Buhl, D., Blenkinsop, J., Veizer, J., 2007. Evolution of the oceanic calcium cycle during the late Mesozoic: evidence from $\delta^{44/40}$Ca of marine skeletal carbonates, *Earth Planet*. Sci. Lett. 253, 96–111.

Fitoussi, C., Bourdon, B., Kleine, T., Oberli, F., Reynolds, B.C., 2008. Si isotopic composition of the Earth's mantle and meteorites. Geochim. Cosmochim. Acta. 71, A273.

Flanagan, F.J., 1967. U.S. Geological Survey silicate rock standards. Geochim. Cosmochim. Acta. 31, 289–308.

Gaetani, G.A., Grove, T.L., 1998. The influence of water on melting on mantle peridotite. Contrib. Miner. Petrol. 131, 323–346.

Galer, S.J.G., O'Nions, R.K., 1989. Chemical and isotopic studies of ultramafic inclusions from the San Carlos Volcanic Field, Arizona: a bearing on their petrogenesis. J. Petrol. 30, 1033–1064.

Georg, R.B., Halliday, A.N., Schauble, E.A., Reynolds, B.C., 2007. Isotopic evidence for silicon in the Earth's core. Nature 447, 1102–1106.

Griffith, E.M., Paytan, A., Caldeira, K., Bullen, T.D., Thomas, E., 2008a. A dynamic marine Ca cycle during the past 28 million years. Science 322, 1671–1674.

Griffith, E.M., Schauble, E.A., Bullen, T.D., Paytan, A., 2008. Characterization of calcium isotopes in natural and synthetic barite. Geochim. Cosmochim. Acta. 72, 5641–5658.

Gussone, N., Böhm, F., Eisenhauer, A., Dietzel, M., Heuser, A., Teichert, B.M.A., Reitner, J., Wörheide, G., Dullo, W.-C., 2005. Calcium isotope fractionation in calcite and aragonite. Geochim. Cosmochim. Acta. 69, 4485–4494.

Hamblock, J.M., Andronicos, C.L., Miller, K.C., Barnes, C.G., Ren, M.-H., Averill, M.G., Anthony, E.Y., 2007. A composite geologic and seismic profile beneath the southern Rio Grande rift, New Mexico, based on xenolith mineralogy, temperature, and pressure. Tectonophysics 442, 14–48.

Handler, M.R., Baker, J.A., Schiller, M., Bennett, V.C., Yaxley, G.M., 2009. Magnesium stable isotope composition of Earth's upper mantle, Earth Planet. Sci. Lett. 282, 306–313.

Hart, S.R., Zindler, A., 1989. Isotope fractionation laws: a test using calcium. Int. J. Mass Spectrom. and Ion Processes 89, 287–301.

Heuser, A., Eisenhauer, A., Gussone, N., Bock, B., Hansen, B.T., Nägler, T.F., 2002. Measurement of calcium isotopes ($\delta^{44/40}$Ca) using a multicollector TIMS technique. Int. J. Mass Spectrom. 220, 387–399.

Heuser, A., Eisenhauer, A., Boehm, F., Wallmann, K., Gussone, N., Pearson, P.N., Naegler, T.F., Dullo, W., 2005. Calcium isotope ($\delta^{44/40}$Ca) variations of Neogene planktonic foraminifera. Paleoceanography 20 (PA2013). doi:10.1029/2004PA001048.

Huang, S., Farkaš, J., Jacobsen, S.B., 2009. Ca isotopic ratios in igneous rocks: some preliminary results. EOS. Trans. AGU, Fall Meet. Suppl. Abstract V11C-1965.

Huang, S., Abouchami, W., Blichert-Toft, J., Clague, D.A., Cousens, B.L., Frey, F.A., Humayun, M., 2009. Ancient carbonate sedimentary signature in the Hawaiian plume: evidence from Mahukona volcano, Hawaii. Geochem. Geophys. Geosyst. 10, Q08002. doi:10.1029/2009GC002418.

Ionov, D., 1998. Trace element composition of mantle-derived carbonates and coexisting phases in peridotite xenoliths from alkali basalts. J. Petrol. 39 (1931–1941), 1998.

Jacobsen, S.B., Kaufman, A.J., 1999. The Sr, C and O isotope evolution of Neoproterozoic seawater. Chem. Geol. 161, 37–57.

Kasemann, S.A., Hawkesworth Ch, J., Pravec, A.R., Fallick, P.N., Pearson, P.N., 2005. Boron and calcium isotope composition in Neoproterozoic carbonate rocks from Namibia: evidence for extreme environmental change Earth Planet. Sci. Lett. 231, 73–86.

Lemarchand, D., Wasserburg, G.J., Papanstassiou, D.A., 2004. Rate-controlled calcium isotope fractionation in synthetic calcite. Geochim. Cosmochim. Acta 68, 4665–4678.

Polyakov, V.B., Clayton, R.N., Horita, J., Mineev, S.D., 2007. Equilibrium iron isotope fractionation factors of minerals: reevaluation from the data of nuclear inelastic resonant X-ray scattering and Mössbauer spectroscopy. Geochim. Cosmochim. Acta. 71, 3833–3846.

Richter, F.M., Watson, E.B., Mendybaev, R., Dauphas, N., Georg, B., Watkins, J., Valley, J., 2009. Isotopic fractionation of the major elements of molten basalt by chemical and thermal diffusion. Geochim. Cosmochim. Acta. 73, 4250–4263.

Rollion-Bard, C., Vigier, N., Spezzaferri, S., 2007. In situ measurements of calcium isotopes by ion microprobe in carbonates and application to foraminifera. Chem. Geol. 244, 679–690.

Russell, W.A., Papanastassiou, D.A., Tombrello, T.A., 1978. Ca isotope fractionation on the Earth and other solar system materials. Geochim. Cosmochim. Acta. 42, 1075–1090.

Salters, V.J.M., Stracke, A., 2004. The composition of the depleted mantle. Geochem. Geophys. Geosyst. 5 (5). doi:10.1029/2003GC000597.

Schauble, E.A., 2004. Applying stable isotope fractionation theory to new systems. In: Johnson, C.M., Beard, B., Albarède, F. (Eds.), Geochemistry of Non-traditional Stable Isotopes: Rev. Mineral. Geochem., 55, pp. 65–111.

Schauble, E. A. in review. First-principles estimates of equilibrium magnesium isotope fractionation in silicate, oxide, and carbonate minerals, *Geochim. Cosmochim. Acta.*

Simon, J.I., DePaolo, D.J., 2010. Stable calcium isotopic composition of meteorites and rocky planets, Earth Planet. Sci. Lett. 289, 457–466. doi:10.1016/j.epsl.2009.11.035.

Skulan, J., DePaolo, D.J., 1999. Calcium isotope fractionation between soft and mineralized tissues as a monitor of calcium use in vertebrates. Proc. Natl. Acad. Sci. 96, 13709–13713.

Skulan, J., DePaolo, D.J., Owens, T.L., 1997. Biological control of calcium isotopic abundances in the global calcium cycle. Geochim. Cosmochim. Acta. 61, 2505–2510.

Smyth, J.R., Bish, D.L., 1988. Crystal Structure and Cation Sites of the Rock Forming Minerals. Allen & Unwin, Boston. 1988.

Tang, J., Dietzel, M., Böhm, F., Köhler, S.J., Eisenhauer, A., 2008. Sr^{2+}/Ca^{2+} and $^{44}Ca/^{40}Ca$ fractionation during inorganic calcite formation: II. Ca isotopes. Geochim. Cosmochim. Acta. 72, 3733–3745.

Teng, F.-Z., Dauphas, N., Helz, R.T., 2008. Iron isotopic fractionation during magmatic differentiation in Kilauea Iki lava lake. Science 320, 1620–1622.

Urey, H.C., 1947. The thermodynamic properties of isotopic substance. J. Chem. Soc. 562–581.

Veizer, J., 1982. Mantle buffering of the early oceans. Naturwissenschaften 69, 173–180.

Williams, H.M., McCammon, C.A., Peslier, A.H., Halliday, A.N., Teutsch, N., Levasseur, S., Burg, J.-P., 2004. Iron isotope fractionation and the oxygen fugacity of the mantle. Science 304, 1656–1659.

Workman, R.K., Hart, S.R., 2005. Major and trace element composition of the depleted MORB mantle (DMM), Earth Planet. Sci.Lett. 231, 53–72. doi:10.1016/j.epsl.2004.12.005.

Wulfsberg, G., 1991. Principles of Descriptive Inorganic Chemistry. University Science Books, Mill Valley, CA. 461 pp.

Yang, W., Teng, F.-Z., Zhang, H.-F., 2009. Chondritic magnesium isotopic composition of the terrestrial mantle: a case study of peridotite xenoliths from the North China craton, Earth Planet. Sci. Lett. 288, 475–482. doi:10.1016/j.epsl.2009.10.009.

Young, E.D., Galy, A., Nagahara, H., 2002. Kinetic and equilibrium mass-dependent isotope fractionation laws in nature and their geochemical and cosmochemical significance. Geochim. Cosmochim. Acta. 66, 1095–1104.

Young, E.D., Tonui, E., Manning, C.E., Schauble, E., Macris, C.A., 2009. Spinel–olivine magnesium isotope thermometry in the mantle and implications for the Mg isotopic composition of Earth, Earth Planet. Sci. Lett. 288, 524–533. doi:10.1016/j.epsl.2009.10.014.

Zheng, Y.F., 1999. Oxygen isotope fractionation in carbonate and sulfate minerals. Geochem.J. 33, 109–126.

Zhu, P., Macdougall, J.D., 1998. Calcium isotopes in the marine environment and the oceanic calcium cycle. Geochim. Cosmochim. Acta. 62, 1691–1698.

Supplemental Material

S1 Ca isotopic analysis by TIMS using GV Isoprobe-T

S1.1 Sample dissolution and ion exchange chemistry

Powdered whole rocks and powdered mineral separates (Table 1) were dissolved in a mixture of 1:1 concentrated HF-HNO_3 acid at 120 °C for 2 days, and mineral crystals and rock chips (Table 1) for 2 weeks. The sample solution was dried down and three times treated with concentrated HNO_3 and once with 6N HCl in order to break insoluble CaF_2. Finally, the sample was re-dissolved in 2.5N HCl, and no residue was observed in any of our samples. From this 2.5N HCl solution, an aliquot of sample solution containing 10-20 μg Ca was pipetted into PFA (Teflon) vial and mixed with appropriate amount of the ^{43}Ca-^{48}Ca double spike solution. The mixtures were left to equilibrate and afterwards dried down and re-dissolved in 10 μL 2.5 N HCl. These solutions were loaded onto Teflon micro-columns filled with 250 μL cation exchange resin BioRad AG50W-X12. Additional 1500 μL 2.5 N HCl was used to rinse the sample into the resin. Following the elution of 1550 μL (Mg, Na, and K), the Ca fraction was collected with additional 1000 μL 2.5 N HCl into a new PFA vial (Fig. S1). After the elution of the Ca fraction, the resin was cleaned with 5000 μL 6N HCl and pre-conditioned with additional 1500 μL 2.5N HCl.

S1.2 Calibration of ion exchange columns

The PFA micro-columns were calibrated by collecting discrete volumes of a calibration solution (a BCR-1 solution) into polyethylene tubes. Approximately 4000 μL 2.5 N HCl were passed through the column and collected in 40 discrete steps of 100 μL each. The concentrations of Ca, Sr, Mg and K of individual elution steps were analyzed by conventional ICP-MS technique and the elemental elution curves are plotted in Fig. S1.

S1.3 Total procedural Ca blank

The Ca blank was determined by conventional isotope dilution technique using a ^{48}Ca spike as a tracer. The total procedural Ca blank was ~25 ng, representing a cumulative contribution of Ca supplied from multiple sources including HNO_3, HF, H_2O, HCl, ion exchange resin, and loading procedure (Re filament and HNO_3). The amount of Ca supplied from the sample was on average 10-20 μg and thus the contribution of Ca from the blank was negligible (<0.3%).

S1.4 Double spike technique and data reduction

The precise measurement of the Ca isotopic ratios in natural samples is possible using a double spike technique, which allows for the correction of isotopic fractionation introduced during the process of chemical preparation and instrumental analysis. The Ca isotope double spike used in this study was prepared from two individual single spike solutions made from isotopically enriched carbonates, Ca43-NX and Ca48-RT, available from Oak Ridge National Laboratory. The Ca43-NX and Ca48-RT carbonates were precisely weighed (±0.003 mg, 2σ) and dissolved in adjusted volumes of 3.5% HNO_3, so

449 the concentration of Ca in the single spike solution would be close to 5 μg per 1000 μL.
450 The Ca isotopic compositions of the ^{43}Ca and ^{48}Ca single spike solutions were
451 determined using total evaporation technique on TIMS and showed only minor (<0.5%)
452 deviations from the certified values (Table S1).

453 The ^{43}Ca and ^{48}Ca single spike solutions were weighed and mixed in such a way
454 that the ^{43}Ca/^{48}Ca ratio in the double spike solution would be close to that of terrestrial
455 materials between 0.7215 and 0.7312 (Russell et al., 1978). The Ca isotopic composition
456 of the double spike solution was determined by TIMS and yielded the ^{43}Ca/^{48}Ca ratio of
457 0.72206. The measured Ca isotopic abundances of the double spike are presented in
458 Table S2.

459 In order to minimize possible contamination from pipette tips, the ^{43}Ca-^{48}Ca
460 double spike solution was kept in a sealed PFA bottle equipped with a special tube that
461 allows a drop-wise addition of the double spike solution to a sample. Approximately 130
462 μL (16 drops) of ^{43}Ca-^{48}Ca double spike solution was added to 20 μg Ca to yield a
463 ^{40}Ca/^{48}Ca ratio (sample to spike ratio) of the mixture close to 60. The double spike
464 solution was added to a sample prior to cation exchange chemistry, so potential isotopic
465 fractionation caused by incomplete recovery of Ca from the columns can be corrected.

466 *S1.5 Mass spectrometry TIMS*

467 The Ca isotopic compositions of standards (NIST SRM 915a and IAPSO
468 seawater) and geological samples were determined at Harvard University using a multi-
469 collector thermal ionization mass spectrometer (TIMS), a GV IsoprobeT instrument.

For the TIMS measurements, the evaporated samples containing about 20 μg of Ca were re-dissolved in 10 μL of 5% HNO_3. From this solution ~5 μg Ca was loaded as calcium nitrate solution directly onto one side filament of a triple Re filament assembly. The solution was slowly, over 10 minutes, dried at a filament current of 0.5 A, then heated at 1.5 A for 1 minute and finally taken to dull red at about 2.2 A for half a minute (Tuttas and Schwieters, 2002).

The instrument was operated in a positive ionization mode with an acceleration voltage of 10 kV and 10^{11} Ω resistor for the Faraday cups. The setup of nine moveable Faraday cups for the Ca isotopic analysis is displayed in Fig. S2. The complete Ca isotope mass range from ^{40}Ca to ^{48}Ca was measured in two sequences. The first sequence collected peaks from ^{40}Ca to ^{44}Ca with ^{41}K on the central cup to monitor a possible isobaric interference of ^{40}K on ^{40}Ca ($^{40}K/^{41}K = 1.7384 \times 10^{-3}$). The second sequence registered isotope peaks from ^{44}Ca to ^{48}Ca with the former on the central cup.

The side filament with a sample was heated to 900 mA and simultaneously the center filament was brought to 3800 mA over about 25 minutes. The beam valve was opened and the ^{40}Ca peak focused and centered. A manual stepwise heating of the side filament continued until reaching a ^{40}Ca beam intensity of about 8 Volts. Prior to data collection, the mass range from 39 to 49 was carefully scanned to check for possible ^{47}Ti and ^{49}Ti peaks and doubly charged ^{87}Sr peak. In all the analyzed samples, no ^{47}Ti, ^{49}Ti or doubly charged ^{87}Sr peaks have been observed. The lack of isobaric interferences in our Ca isotopic analysis is also corroborated in three Ca isotope plots (Fig. 3), where all the measured samples plot along the mass-dependent exponential fractionation lines. During

492 data collection, the vacuum in the ion source and analyzer was below 1 x 10^{-7} and 3 x 10^{-9}
493 mbar, respectively. Baselines were measured at mass 46.5 for 30 seconds before each
494 block. Checks of the baselines and peaks showed that there were no reflected ions or
495 electrons perturbing measurements. Each analysis consisted of 20 blocks, 10 cycles each,
496 using a 6-second integration time for each sequence, followed by a 1-second waiting time.
497 A total analytical time for an individual measurement was approximately 120 minutes,
498 including the 25-minute heating routine. Typically, the in-run instrumental isotopic
499 fractionation for $^{44}Ca/^{40}Ca$ was less than 0.5 per mil (2σ).

500 *S1.6 Iterative double spike correction algorithm*

501 The $^{44}Ca/^{40}Ca$ ratio of a sample was calculated from the raw $^{40}Ca/^{48}Ca$, $^{43}Ca/^{48}Ca$
502 and $^{44}Ca/^{48}Ca$ ratios in a spiked sample applying an iterative routine based on algorithm
503 with an exponential fractionation term adopted from Heuser et al. (2002), using Ca
504 isotopic composition of our double spike solution and the "Russell values" as the starting
505 Ca isotopic ratios (Table S2). The fractionation corrected $^{44}Ca/^{40}Ca$ ratio in the original
506 sample was converted to delta notation ($\delta^{44/40}Ca$) in per mil (‰) relative to the NIST
507 SRM 915a $CaCO_3$ standard using the following relation:

508 $$\delta^{44/40}Ca = \left(\frac{^{44}Ca/^{40}Ca_{SAMPLE}}{^{44}Ca/^{40}Ca_{SRM\,915a}} - 1 \right) \cdot 1000 \text{, where } ^{44}Ca/^{40}Ca_{\text{SRM 915a}} = 0.021549.$$

509 **S2 Are the High $\delta^{44/40}Ca$ in Orthopyroxenes an Analytical Artifact?**

510 The most exciting finding of this study is the high $\delta^{44/40}Ca$ in mantle
511 orthopyroxenes. Could this be an analytical artifact?

512 Russell and Papanastassiou (1978) showed that Ca isotopes are fractionated on
513 the cation columns; consequently, 100% yield of Ca is necessary for correctly
514 determining the stable isotopic ratios of Ca, if the sample is not spiked prior to column
515 chemistry. However, we applied a double spike technique, in which samples were spiked
516 with mixed ^{43}Ca-^{48}Ca spike solution (^{43}Ca/^{48}Ca = 0.72206) before loaded on the columns.
517 Consequently, any possible isotopic fractionation caused by the column chemistry can be
518 corrected. In addition, our columns have been carefully calibrated (Fig. S1) to ensure
519 100% yield. In Fig. S3, the $\delta^{44/40}$Ca, which were corrected for instrumental isotopic
520 fractionation, are plotted against the raw ^{43}Ca/^{48}Ca and raw ^{40}Ca/^{48}Ca. The ^{43}Ca/^{48}Ca in
521 the spiked samples is dominated by the ^{43}Ca/^{48}Ca from the spike solution, because ~90%
522 of ^{43}Ca and ^{48}Ca in the mixtures (spiked samples) come from spike solution. The scatter
523 of the raw ^{43}Ca/^{48}Ca in measured samples reflects variant ^{43}Ca-^{48}Ca contributions from
524 samples and instrumental isotopic fractionation. The limited range in raw ^{43}Ca/^{48}Ca
525 (0.718-0.722) implies that Ca isotopes were not fractionated on the columns. If the high
526 $\delta^{44/40}$Ca in orthopyroxenes were caused by incomplete column yields, a negative raw
527 ^{43}Ca/^{48}Ca-δ^{44}Ca/^{40}Ca trend should be expected, because columns preferentially hold light
528 Ca isotopes (Russell and Papanastassiou, 1978). However, such trends are not observed
529 (Fig. S3a). Rather, the $\delta^{44/40}$Ca shows no correlation with either raw ^{43}Ca/^{48}Ca or raw
530 ^{40}Ca/^{48}Ca, the latter reflects the sample to spike ratio. Consequently, the high $\delta^{44/40}$Ca in
531 orthopyroxenes are not an analytical artifact of incomplete column yield or inappropriate
532 sample to spike ratio.

533 Could the high $\delta^{44/40}$Ca in orthopyroxenes be caused by isobaric interferences?
534 ^{40}K interferes on ^{40}Ca, and in our analytical procedure ^{41}K is monitored to correct for ^{40}K

535 interference on ^{40}Ca. Since K evaporates at lower temperature than Ca, K interference is
536 not a serious problem in our Ca isotopic analysis. Typically, the ^{40}K interfere correction
537 on ^{40}Ca is less than 10 ppm; thus the high $\delta^{44/40}$Ca in orthopyroxenes cannot be caused by
538 a K interference.

539 Also no doubly charged Sr ions that could interfere on Ca isotopes (e.g. ^{88}Sr on
540 ^{44}Ca) were observed. This was checked by monitoring mass 43.5 (i.e. doubly charged
541 ^{87}Sr) prior to data collection.

542 ^{48}Ti interferes on ^{48}Ca. We do not monitor a Ti isotope during data acquisition.
543 However, we scan the mass range from 39 to 49 checking for possible ^{47}Ti and ^{49}Ti peaks
544 before starting to collect data. In all the analyzed samples, including the orthopyroxene
545 samples, and standards, no ^{47}Ti or ^{49}Ti peaks have ever been observed. Further more, any
546 ^{48}Ti interference on ^{48}Ca leads to lower, rather higher, $\delta^{44/40}$Ca. So, the high $\delta^{44/40}$Ca in
547 orthopyroxenes is not caused by a Ti interference.

548 In addition, the fact that all our measured samples plot along the theoretically
549 calculated mass-dependent exponential fractionation lines in three Ca isotope plots (Fig.
550 3) rules out the presence of isobaric interferences in our Ca isotopic measurements.

551

552 Could the high $\delta^{44/40}$Ca in orthopyroxenes be caused by preferentially leaching
553 light Ca isotopes out of orthopyroxene during the 1N HCl leaching step? Powdered San
554 Carlos clinopyroxene and orthopyroxene separates were used in our leaching experiments
555 (Table 1). In our leaching experiment, the acid-to-sample Ca ratios are very large. In
556 particular, 13 mg of clinopyroxene powder and 43 mg of orthopyroxene powder were
557 leached with 6 ml 1N HCl. Consequently, if the high $\delta^{44/40}$Ca in San Carlos

558 orthopyroxene is caused by reaction with 1N HCl, a similar effect should be observed on
559 San Carlos clinopyroxene. However, 1N HCl leaching does not affect the $\delta^{44/40}$Ca in San
560 Carlos clinopyroxene powder (see **Section 3**).

561 In fact, even the unleached San Carlos orthopyroxene has distinctively heavier Ca
562 isotopes than average basalt and clinopyroxenes (Table 1). This difference is clearly
563 shown in a three Ca isotope plot, $\delta^{44/40}$Ca vs. $\delta^{44/42}$Ca (Fig. 3).

564 Further evidence comes from our measurements of Kilbourne Hole orthopyroxene.
565 Unlike the San Carlos peridotite case, we analyzed mm to sub-mm size orthopyroxene
566 crystals for Kilbourne Hole peridotite (Table 1). Although these mm to sub-mm size
567 Kilbourne Hole orthopyroxene crystals were leached with 1N HCl at room temperature
568 for overnight, it is unlikely that such a weak acid leaching is able to modify the Ca
569 isotopic ratios in these crystals. Moreover, if the 1N HCl leaching step would increase
570 $\delta^{44/40}$Ca in orthopyroxenes, one would expect a bigger effect on the leached San Carlos
571 orthopyroxene powder than that on the leached mm to sub-mm size Kilbourne Hole
572 orthopyroxene crystals, since the latter have much smaller surface areas. However,
573 Kilbourne Hole orthopyroxene has a significantly higher $\delta^{44/40}$Ca than San Carlos
574 orthopyroxene (Table 1; Fig. 2), which argues against the possibility that acid leaching is
575 responsible for the high $\delta^{44/40}$Ca in orthopyroxene.

576 In summary, the observed high $\delta^{44/40}$Ca in orthopyroxene separates from San
577 Carlos and Kilbourne Hole mantle peridotites are not analytical artifacts.

578

579

580